TR/99 May 1980

The use of splines and singular functions in an integral equation method for conformal mapping.

by

D. M. Hough * and N. Papamichael

* Division of Mathematics, Polytechnic of the South Bank, Wandsworth Road, London SW8 2JZ.

ABSTRACT

We consider the integral equation method of Symm for the conformal mapping of simply-connected domains. For the numerical solution, we examine the use of spline functions of various degrees for the approximation of the source density σ. In particular, we consider ways for overcoming the difficulties associated with corner singularities. For this we modify the spline approximation and in the neighbourhood of each corner, where a boundary singularity occurs, we approximate σ by a function which reflects the main singular behaviour of the source density. The singular functions are then blended with the splines, which approximate σ on the remainder of the boundary, so that the global approximating function has continuity of appropriate order at the transition points between the two types of approximation. We show, by means of numerical examples, that such approximations overcome the difficulties associated with corner singularities and lead to numerical results of high accuracy.

1. Introduction

This paper is concerned with the problem of determining approximations to the function f which maps conformally a bounded simply-connected domain onto the unit disc. There are several numerical methods for approximating f and most of these are described in the book of Gaier [2], which is devoted entirely to numerical conformal mapping techniques. Here we consider the integral equation method of Symm [13], which has received considerable attention recently; see Hayes, Kahanner and Kellner [5,6] Gaier [4], Jaswon and Symm C9], Henrici [7] and Wendland [16].

Let Ω be a bounded simply-connected domain in the complex z-plane whose boundary $\partial\Omega$ is a rectifiable Jordan curve with parametric equation $z = \zeta(t)$ where t, $0 \leq t \leq \ell$, is the arc length. Assume, without loss of generality, that the origin of co-ordinates 0 lies in Ω and let f be the function which maps Ω conformally onto the unit disc

$$D = \{w : |w| < 1\} ,$$

so that $f(0) = 0$. Then,

$$f(z) = z \exp\{g(z) + ih(z)\} , \qquad z \in \bar{\Omega} \equiv \Omega \cup \partial\Omega , \tag{1.1}$$

where the functions g and h are real valued harmonic conjugates and g satisfies the boundary condition

$$g(z) = -\log|z| , \quad z \in \partial\Omega . \tag{1.2}$$

The method of Symm [13] consists of expressing the harmonic function g as a single layer potential

$$g(z) = \int_{\partial\Omega} \log|z - \zeta| \, \sigma(\zeta) \, dt , \tag{1.3}$$

where a is an unknown source density. The conjugate function h is then given by

$$h(z) = \arg \left\{ \frac{f(z)}{z} \right\}$$

$$= \int_{\partial\Omega} \arg |z- \zeta | \sigma (\zeta) \quad dt , \qquad (1.4)$$

and the boundary condition (1.2) gives

$$\int_{\partial\Omega} 1\log |z- \zeta | \sigma (\zeta) \, dt = -\log ,|z| , \qquad z \in \partial \Omega . \qquad (1.5)$$

In this way the mapping problem is reduced to the solution of equation (1.5), which is a Fredholm integral equation of the first kind in σ. Once σ is found, g and h are determined from (1.3) and (1.4), and finally (1.1) gives the mapping function f at any point $z \varepsilon \Omega$ If f is required at boundary points only then the conjugate function h can be determined by simple integration of as follows. Let θ be the boundary correspondence function, i. e.,

$$\theta (t) = \arg\{f(\zeta(t))\} \quad . \qquad (1.6)$$

Then, it can be shown that

$$\sigma = - \frac{1}{2\pi} \frac{d\theta}{dt} \qquad (1.7)$$

Thus 0 and hence h can be found at a boundary point by using (1.7), instead of (1.4). The result (1.7) is due to Gaier [4]. Another immediate consequence of this result is that

$$\int_0^{\ell} \sigma (\zeta) dt = -1 . \qquad (1.8)$$

The question of existence and uniqueness of solution of the integral equation (1.5) is considered fully in Gaier [4], It turns out that (1.5) has a unique solution provided that the transfinite diameter associated with $\partial\Omega$, is not equal to unity. This implies that a unique

solution of (1.5) always exists, subject only to a possible rescaling of Ω; see also Jaswon and Symm [9,p.61]. Alternatively, the integral equation (1.5) slightly modified and coupled with equation (1.8) provides a system which always has a unique solution. This alternative was proposed recently by Wendland [16].

For the numerical solution of (1.5), Symm [13] approximates the Source density a by a step function, and determines this approximation by collocation at an appropriate number of boundary points. Hayes et al [5] obtain a numerical solution of (1.5) in a similar manner, by approximating σ by a C^o piecewise defined quadratic polynomial. Both these numerical techniques have been successfully tested and, as might be expected, the technique of [5] leads to considerable improvement in accuracy. However, if $\overline{\Omega}$ contains corners then σ may have singularities which affect the accuracy of the approximation. In particular, at a re-entrant corner σ becomes unbounded and this singularity of the source density has a serious damaging effect on the accuracy of the approximate mapping function, especially in the neighbourhood of the corner. An indication of this damaging effect is given by the results of Symm [14,p.293] and Gaier [4,p.128], who consider the conformal mapping of an L—shaped region.

In the present paper we consider the conformal mapping of polygonal domains and examine the use of spline functions of various degrees for the approximation of a. However, our main purpose is to consider ways for overcoming the difficulties associated with corner singularities. For this we modify the spline approximation, and in the neighbourhood of each corner where a boundary singularity occurs we approximate σ by a function which reflects the main singular behaviour of the source

density. The singular functions are then blended with the splines, which approximate a on the remainder of the boundary, so that the global piecewise defined approximating function has continuity of appropriate order at the transition points between the two types of approximation. We show, by means of numerical examples, that such approximations to σ overcome the difficulties associated with corner singularities and lead to numerical results of high accuracy.

2. Singularities in the source density

Let $w = f(z)$ be the conformal map. Then the boundary correspondence function (1.6) is given by

$$\theta = I(\log \overline{w} - \log w)/2 \quad ; \qquad z \in \partial\Omega \ . \tag{2.1}$$

Since $|w| = 1$ for $z \in \partial\Omega$, it follows from (1.7) that

$$\sigma = i\left\{\overline{w}\frac{\partial w}{\partial t} - w\frac{\partial \overline{w}}{\partial t}\right\}/4\pi. \tag{2.2}$$

Let z be a corner of the polygonal domain Ω with interior angle $\alpha\pi$; $0 < \alpha < 2$. Then it follows from the Schwarz-Christoffel formula that in the neighbourhood of (z_o)

$$f(z) = f(z_o) + \sum_{j=1}^{\infty} A_j (z - z_o)^{j/\alpha}; \tag{2.3}$$

see, e.g., Copson [1,p.170]. For any point $z = \zeta(t)$ on the arms of the corner we may take, without any loss in generality,

$$z - z_0 = \begin{cases} t - t_0 \ , & t \geq t_0 \ , \\ t_0 - t)\ \exp(i\alpha\pi) \ , & t < t_0 \ . \end{cases} \tag{2.4}$$

Thus, (2.2), (2.3) and (2.4) imply that

$$\sigma = \begin{cases} \sum_{j=1}^{\infty} a_j (t-t_0)^{-1+j/\alpha}, & t \geq t_0, \\ \sum_{j=1}^{\infty} (-1)^{1+j} a_j (t-t_0)^{-1+j/\alpha}, & t > t_0, \end{cases} \tag{2.5}$$

where

$$a_j = (2\pi\alpha)^{-1} \operatorname{Im} \left\{ \sum_{r=1}^{j} r A_{j-r} \overline{A}_r \right\}, \tag{2.6}$$

with $A_0 = f(z_0)$.

Let $\sigma^{(r)} = d^r \sigma / dt^r$. Then the following conclusions can be drawn from (2.5) :

(i) If $\alpha = 1/q$, where $q \geq 1$ is an integer, then (2.5) does not involve fractional powers of $t - t_0$ and,

(a) if q is odd then there are no singularities in σ at $t = t_0$,

(b) if q is even then, in general, $\sigma^{(q-1)}$ has a finite jump discontinuity at $t = t_0$.

(ii) If $1/(q+1) < \alpha < 1/q$, where $q \geq 1$ is an integer, then $\sigma^{(q)}$ becomes unbounded at $t = t_0$.

(iii) If $1 < \alpha < 2$, i.e. the corner is re—entrant, then σ itself becomes unbounded at $t = t_0$.

3. The Numerical Method

Over most of $\partial\Omega$,σ is approximated by spline functions of the same degree n. However, in the neighbourhood of a corner point z_o with interior

angle $\alpha\pi$, where singularities of the type described in Section 2 occur, one of the fo1lowing two procedures is used:

(a) the spline approximation is continued through z_o ,

or

(b) a special function which reflects the known asymptotic behaviour of σ near z_o is used to approximate σ in the neighbourhood of this point .

If procedure (b) is used then the special function is blended with the spline approximation by imposing appropriate continuity conditions at the transition points between the two types of approximation. In this case we call the resulting approximating function an "augmented spline" of degree n.

Wnether procedure (a) or (b) is used depends on the nature of the singularity in σ and on the degree of the splines approximating σ over the rest of the boundary. For example, if $a > 1$, i.e. the corner is re-entrant and a is unbounded at z_o , then procedure (b) should always be used. However, at a right angled corner, where the singularity is a jump discontinuity in $\sigma^{(1)}$, a suitable approach might be to use procedure (a) for splines of degree 0 or I and procedure (b) for splines of higher degree. Clearly the above scheme contains as special cases the use of a global spline approximation over the whole boundary and the use of an approximation which employs special functions at every corner of the polygon.

We now describe the computational details of the numerical method for the augmented spline approximation. For this, it is convenient to allow the parameter t to take any real values and to regard σ as a periodic function of t with period ℓ .

Let the corner points of $\partial\Omega$ at which procedure (b) is to be used be called the "singular corner points" and assume that there are $N \geq I$ such points with arc lengths $t = \tau_I$; I = 1 (1)N, where $0 < \tau_1 < \tau 2 < \ldots < \tau_N < \ell$. Let $[\tau_I, \tau_{I+1}]$; I = 1(1)N, be divided into $k_I + 3$; I = 1(1)N, intervals, where $k_I > 0$ and $\tau_{N+1} = \tau_1 + \ell$ The endpoints of these intervals are denoted by t_{Ij} where

$$\tau_I = t_{I0} < t_{I1} < \ldots < t_{I,k_I+3} = \tau_{I+1};\ I = 1\ (1)\ N. \tag{3,1}$$

It is also convenient to introduce the following additional notation ,

$$\left.\begin{aligned} t_{1,-1} &= t_{N,\ k_N+2} - \ell \\ t_{I,-1} &= t_{I-1,k_{I-1}+2};\quad I = 2\ (1)\ N. \end{aligned}\right\} \tag{3.2}$$

We assume that the arc length of every corner point of $\partial\Omega$ is an endpoint in the list (3.1), and note that the intervals defined by (3-1) need not be of the same length.

The source density σ is approximated by

$$\tilde{\sigma}(t) = \begin{cases} r_I(t),\ t_{I,-1} < t < t_{I1}, \\ s_I(t),\ t_{I1} < t < t_{I,k_I+2};\ I = 1(1)\ N, \end{cases} \tag{3.3}$$

where s_I is a spline of degree n with knots t_{Ij} ; $j = 1\ (1)k_I + 2$, and r_I is an appropriate singular function. More specifically, if the singular corner point at $\tau_I = t_{I0}$ has an interior angle $\alpha_I \pi$ then we truncate the series (2.5) and take

$$r_I(t) = \begin{cases} \sum_{j=1}^{m_I} a_{Ij}\ (t - t_{I0})^{-1+j/\alpha_I},\ t_{I0} \leq t < t_{I1} \\ \sum_{j=1}^{m_I} (-1)^{1+j}\ a_{Ij}\ (t_{I0} - t)^{-1+j/\alpha_I},\ t_{I,-1} < t \leq t_{I0}\ . \end{cases} \tag{3.4}$$

For s we use the truncated power function representation

$$s_I(t) = \sum_{j=0}^{n} b_{Ij}(t - t_{I1})j + \sum_{j=2}^{k_I+1} c_{Ij}(t - t_{Ij})_+^n, \tag{3.5}$$

where

$$(t - t_{Ij})_+ = \begin{cases} t - t_{Ij}, & t > t_{Ij}, \\ 0, & t > t_{Ij}. \end{cases} \tag{3.6}$$

It is clear from (3.3), (3.4) and (3.5) that the total number of unknown parameters involved in the approximating function $\tilde{\sigma}$ is

$$M_0 = (n+1)N + \sum_{I=1}^{N} (k_I + m_I). \tag{3.7}$$

We determine these parameters by collocating at a number of points on $\partial\Omega$ and also by imposing certain continuity conditions on $\tilde{\sigma}$. We first describe the formation of the collocation equations.

For splines of odd degree n we collocate at the endpoints (3.1) of each interval on $\partial\Omega$. For splines of even degree n we collocate at the midpoints of each of these intervals. We have found that this choice of collocation points allows us more easily to take advantage of any symmetry of Ω in order to reduce the number of collocation equations. In general, denote the collocation points by z_i; $i = 1(1)M_1$, where from (3.1),

$$M_1 = 3N + \sum_{I=1}^{N} k_I. \tag{3.8}$$

Then, from (1.5), the collocation equations are

$$\int_0^{\ell} \tilde{\sigma}(t) \log |z_i - \varsigma(t)| dt = -\log |z_i|; i = I(I)M_I \tag{3.9}$$

or, using (3.3), (3.4), (3-5) and (3.6),

$$\left.\sum_{I=1}^{N} \left[\sum_{j=1}^{mI} A_{Iij} a_{Ij} + \sum_{j=0}^{n} B_{Iij} b_{Ij} + \sum_{j=2}^{kI+1} C_{Iij} c_{ij} \right] = -\log |z_i|; \right\} \quad i = 1(1)m1, \tag{3.10}$$

where

$$\left.\begin{aligned} A_{Iij} &= (-1)^{1+j}\int_{tI,-1}^{t10}(t_{10}-t)^{-1+j/\alpha/}\log|z_i-\varsigma(t)|\,dt \\ &\quad+\int_{t_{I0}}^{t_{I1}}(t-t_{10})^{-1+j/\alpha_I}\log|z_i-\varsigma(t)|\,dt, \\ B_{Iij} &= \int_{t_{Ij}}^{t_{I,k_I+2}}(t-t_{Il})^{j}\log|z_i-\varsigma(t)|\,dt, \\ C_{Iij} &= \int_{t_{Ij}}^{t_{I,k_I+2}}(t-t_{Ij})^{n}\log|z_i-\varsigma(t)|\,dt. \end{aligned}\right\} \quad (3.11)$$

We now consider the continuity conditions on $\tilde{\sigma}$. Assume that at the transition points $t_{I-1.}$, and $t_{I1,,}$ where the type of approximation changes, the first d_I derivatives of $\tilde{\sigma}$ are required to be continuous. These requirements imply

$$r_I^{(k)} = \begin{cases} s_I^{(k)} \text{ at } t = t_{I1}\,; I = 1(1)N, \\ s_{I-1}^{(k)} \text{ at } t = t_{I,-1}\,; I = 2(1)N, \\ s_N^{(k)}(t_{N,k_N+2}) \text{ at } t = t_{1,-1},\ k = 0(1)d_I, \end{cases} \quad (3.12)$$

and, on using (3.4) and (3.5), lead to the M_2 continuity equations

$$\left.\begin{aligned} &\sum_{j=1}^{m_I} a_{Ij}(-1+j/\alpha_I)(-2+j/\alpha_I)\ldots(-k+j/\alpha_I)(t_{I1}-t_{I0})^{-1-k+j/\alpha_I} = b_{Ik}k!\,, \\ &\sum_{j=1}^{m_I} a_{Ij}(-1)^{1+j+k}(-1+j/\alpha_I)(-2+j/\alpha_I)\ldots(-k+j/\alpha_I)(t_{I0}-t_{I,-1})^{-1-k+j/\alpha_I} \\ &\quad=\sum_{j=0}^{n} b_{I-1,j}j(j-1)\ldots(j-k+1)(t_{I,-1}-t_{I-1,1})^{j-k} \\ &\quad+\sum_{j=2}^{k_{I-1}+1} c_{I-1,j}n(n-1)\ldots(n-k+1)(t_{I,-1}-t_{I-1,j})^{n-k}; \\ &\qquad\qquad I=1(1)N, k=0(1)d_I, \end{aligned}\right\} \quad (3.13)$$

where $b_{0j} = b_{Nj}$, $c_{0j} = c_{Nj}$, $t_{0j} = t_{Nj} - \ell$ and

$$M_2 = 2 \sum_{I=1}^{N} (1 + d_I) \quad . \tag{3.14}$$

To determine the parameters of $\tilde{\sigma}$ we require that $M_o = M_1 + M_2$, i.e. from (3.7), (3-8) and (3.14),

$$2 \sum_{I=1}^{N} d_I = N(n - 4) + \sum_{I=1}^{N} m_I \tag{3.15}$$

The equations (3.10) and (3.13) then constitute an M_o x M_o linear system which is solved for the M_o unknown parameters a_{IJ} , b_{Ij}. and c_{Ij} .

A sufficient condition for (3.15) to hold is that

$$2d_I = n + m_I - 4 \; ; \quad I = 1(1)N \quad . \tag{3.16}$$

For this reason we always take $n + m_I$ to be an even number which satisfies (3.16). Since $m_I > 0$, this implies that $d_I \geq -I$ always, (Here, $d_{I=-1}$ corresponds to a jump discontinuity in σ at the transition points $t_{I,-1}$, t_{I1}). Also, since a spline of degree n is in the continuity class C^{n-1}, it is reasonable to require that

$$d_I \leq n - 1 \; ; \quad I = 1(1)N \quad , \tag{3.17}$$

which, from (3.16), is equivalent to the requirement

$$m_I < n + 2 \; ; \; I = 1(1)N \quad . \tag{3.18}$$

Clearly, for a given degree of spline n there may be several possible choices for either m_I or d_I, within the framework of the above restrictions .

Once the M parameters a_{Ij} , b_{Ij} , and c_{Ij}. are computed, the approximate mapping function $\tilde{f}(z)$ is determined from (1.1) by evaluating

$$\tilde{g}(z) + i\tilde{h}(z) = \int_0^{\ell} \tilde{\sigma}(t) \log(z - \zeta(t)) \, dt \quad , \tag{3.19}$$

where $\log(z-\zeta(t)) = \log|z-\zeta(t)| + i\arg(z-\zeta(t))$. Using (3.3), (3.4) and (3.5) in (3.19) we find

$$\tilde{g}(z) + i\tilde{h}(z) = \sum_{I=1}^{N} \left(\sum_{j=1}^{m_I} a_{Ij} A_{Ij}(z) + \sum_{j=0}^{n} b_{Ij} B_{Ij}(z) + \sum_{j=2}^{k+1} c_{Ij} C_{Ij}(z) \right), \quad (3,20)$$

where

$$\left.\begin{aligned} A_{Ij}(z) &= (-1)^{1+j} \int_{t_{I,-1}}^{t_{I0}} (t_{I0} - t)^{-1+j/\alpha_I} \log(z - \zeta(t))dt \\ &\quad + \int_{t_{I0}}^{t_{I1}} (t - t_{I0})^{-1+j/\alpha_I} \log(z - \zeta(t))dt , \\ B_{Ij}(z) &= \int_{t_{I1}}^{t_{I,k_I+2}} (t - t_{Il})^{j} \log(z - \zeta(t))dt , \\ C_{Ij}(z) &= \int_{t_{Ij}}^{t_{I,k_I+2}} (t - t_{Ij})^{n} \log(z - \zeta(t))dt . \end{aligned}\right\} \quad (3.21)$$

The coefficients (3-11) in the collocation equations(3.10) are related to the functions (3.21) by

$$A_{Iij} = \mathrm{Re}\{A_{Ij}(z_i)\} , \quad B_{Iij} = \mathrm{Re}\{B_{Ij}(z_i)\} , \quad C_{Iij} = \mathrm{Re}\{C_{Ij}(z_i)\} . \quad (3.22)$$

For the polygonal domains considered in this paper, the integrals (3.21) and (3.22) are computed from the exact formulae which are derived in Hough [8].

The computational details for the global spline approximation are clearly analogous to those of the "augmented splines" given above. The only change in the above numerical procedure concerns the continuity conditions (3.12) which, in the case of a global spline approximation, must be replaced by appropriate periodic end conditions.

4. Numerical Examples

In this section the integral equation method is applied to a number of polygonal domains. In all examples the maximum error in the modulus of the computed mapping function is estimated by

$$\varepsilon_{\text{mod}} = \max_{i=1(1)M_1} \left| 1 - |\tilde{f}(z_{i+\frac{1}{2}})| \right| . \tag{4.1}$$

In (4.1) M_1 is the number of collocation points used, and $z_{i+\frac{1}{2}} \in \partial\Omega$ are either interval end points or midpoints, depending on whether the degree of splines used is even or odd. That is, each test point $z_{i+\frac{1}{2}}$ always lies between successive collocation points and, in almost all cases, is midway between the collocation points. For each example we compare our numerical results with either values computed from the exact mapping or values obtained by other numerical methods. In examples for which the exact mapping function is known the maximum error in the argument of the computed map is estimated by

$$\varepsilon_{\arg} = \max_{i=1(1)M_1} \{ |\arg f(z_i) - \arg \tilde{f}(z_i)|, |\arg f(z_{i+\frac{1}{2}}) - \arg \tilde{f}(z_{i+\frac{1}{2}})| \}. \tag{4.2}$$

In presenting our results we use the notation m_A., m_B, m_C, . . . , to denote the number of terms used in the truncated series (3.4) at corner points labelled A, B, C,… . In using this notation we take $m_p = 0$ to mean that corner point P is not taken to be a "singular corner".

In all examples we make full use of any symmetry in $\partial\Omega$ so as to reduce the size of the linear system. If symmetry is used then we take M_1^* and M_0^* to denote respectively the number of collocation equations formed and the total number of equations solved.

The computations were carried out on a DEC 10 computer, using programs written in DEC 10 Algol with double precision working. Single length working is between 8 and 9 significant figures .

Example 1

Rectangles $\Omega_a \equiv \{(x,y) : |x| < 1, |y| < a\}$; $a = 1,\ 0.5,\ 0.2,\ 0.1$.

In this case the exact mapping function is known in terms of Jacobian elliptic functions ; see, e.g. Milne-Thomson [11] .

The corner points are

$$A : 1 + ia , \quad B : -1 + ia , \quad C : -1 - ia , \quad D : 1 - ia$$

and we take

$$^{m}A = {}^{m}B = {}^{m}C = {}^{m}D = m .$$

In the numerical method we take $M_I = 128$. The M_1. intervals used are of uniform length on any given side of Ω_a and their actual distribution is shown in Table 1 (a). Because of the symmetry of Ω_a the number of collocation equations and the total number of equations solved can be reduced respectively to M_1^* , M_0^* where

$$M_1^* = \begin{cases} 17, & n \quad \text{odd} \\ 16, & n \quad \text{even} \end{cases} \Bigg\} \; a = 1 \ , \qquad \begin{cases} 33, & n \quad \text{odd} \\ 32, & n \quad \text{even} \end{cases} \Bigg\} \; a \neq 1 \ ,$$

$$M_0^* = \begin{cases} M_1^* + [n/2] + [m/2] + (n+m)/21, & m \neq 0 \text{anda} = 1, \ m \neq 0 \text{anda} = 1, \\ M_1^* + 2[n/2] + n + m - 2 & , m \neq 0 \text{anda} \neq 1, \\ M_1^* + 2[n/2] & , m = 0 \quad , \end{cases}$$

and [.] denotes the integer part .

The numerical results are presented in Tables 1(b), 1(c), 1(d), 1(e) and 1(f), For the augemented spline results all possible values of m, subject to the restriction (3.18), are considered for each value of n. For a= 1, 0.5, 0.2 the results presented in Tables 1(b), 1(c), 1(d) correspond to those values of m which give the best accuracy, in the sense that increasing m beyond the values indicated leaves ε_{mod} and ε_{arg} unnaltered.

When $a = 0.1$, the values of ε_{mod}.. and ε_{arg} obtained by using augmented splines are exactly the same as those of the global splines given in Table 1(e), irrespective of the value of m. Furthermore, these maximum errors always occur in the neighbourhood of the points $z = \pm$ ia. This can be explained as follows. The magnitude of the jump discontinuity in $\sigma^{(1)}$ at a corner decreases as a decreases. For example, from our computed solutions with $n = 5$ and $m = 3$ we find that at a corner, where $t = t_0$,

$$|\tilde{\sigma}^{(1)}(t_0+) - \tilde{\sigma}^{(1)}(t_0-)| = \begin{cases} 5.5 \times 10^{-1}, & a = 1, \\ 5.4 \times 10^{-1}, & a = 0.5, \\ 3.0 \times 10^{-2}, & a = 0.2, \\ 4.7 \times 10^{-5}, & a = 0.1. \end{cases}$$

Thus, it appears that the corner point singularity is not a source of computational difficulty for small a. The difficulty in the case $a = 0.1$ concerns the fact that the mapping function $w = f(z)$ has poles at $z = \pm 2$ ia; see Levin, Papamichael and Sideridis [10]. This implies that a and its derivatives $\sigma^{(n)}$ have large magnitudes in the neighbourhood of $z = \pm$ ia. The above can be established from (1.7) and the Cauchy-Riemann equations since, on $y = + a$,

$$\sigma = \pm \frac{1}{2\pi} \frac{\partial \Theta}{\partial x} = \mp \frac{1}{2\pi} \frac{\partial \log |w|}{\partial y} .$$

To illustrate how σ behaves as a decreases we present, in Figure 1, sketches of ex corresponding to global linear spline approximations. These indicate that a spline with uniformly spaced knots may not be able to approximate σ adequately for small values of a. For this reason, when a=0.1, we take M, = 128 and use a simple non-uniform interval distribution, such that the interval lengths decrease in arithmetic progression towards the midpoint of a longer side. This distribution is suggested by Symm [15]. The results of this experiment are given in Table 1(f) .

Table 1(a)

Number of intervals per side ,

a	AB, CD	AD,BC
1	32	32
0.5	44	20
0.2	54	10
0.1	58	6

Table 1(b)

a = 1

n	Global Spline		Augmented Spline		m
	ε_{mod}	ε_{arg}	ε_{mod}	ε_{arg}	
0	4×10^{-4}	3×10^{-4}	2×10^{-4}	3×10^{-4}	2
1	9×10^{-6}	3×10^{-6}	9×10^{-6}	3×10^{-6}	1
2	2×10^{-4}	1×10^{-4}	4×10^{-8}	1×10^{-7}	2
3	9×10^{-5}	7×10^{-5}	9×10^{-9}	5×10^{-9}	3
4	2×10^{-4}	1×10^{-4}	2×10^{-10}	3×10^{-10}	4
5	1×10^{-4}	8×10^{-5}	3×10^{-11}	2×10^{-11}	3

Table 1(c)

a = 0.5

n	Global Spline		Augmented Spline		m
	ε_{mod}	ε_{arg}	ε_{mod}	ε_{arg}	
0	2×10^{-4}	4×10^{-4}	1×10^{-4}	4×10^{-4}	2
1	2×10^{-5}	1×10^{-5}	2×10^{-5}	1×10^{-5}	1
2	1×10^{-4}	7×10^{-5}	3×10^{-7}	5×10^{-7}	2
3	6×10^{-5}	4×10^{-5}	6×10^{-8}	4×10^{-8}	3
4	1×10^{-4}	6×10^{-5}	3×10^{-9}	3×10^{-9}	2
5	7×10^{-5}	5×10^{-5}	5×10^{-10}	4×10^{-10}	3

Table 1(d)

a = 0.2

n	Global Spline		Augmented Spline		m
	ε_{mod}	ε_{arg}	ε_{mod}	ε_{arg}	
0	4×10^{-4}	2×10^{-3}	4×10^{-4}	2×10^{-3}	2
1	2×10^{-4}	1×10	2×10^{-4}	1×10^{-4}	1
2	1×10^{-5}	1×10^{-5}	1×10^{-5}	1×10^{-5}	2
3	3×10^{-6}	2×10^{-6}	3×10^{-6}	2×10^{-6}	1
4	5×10^{-6}	2×10^{-6}	6×10^{-7}	4×10^{-7}	2
5	2×10^{-6}	2×10^{-6}	1×10^{-7}	2×10^{-7}	3

Table 1 (e)

a = 0.1

n	Global	Spline
	ε_{mod}	ε_{arg}
0	3×10^{-3}	5×10^{-3}
1	1×10^{-3}	1×10^{-3}
2	3×10^{-4}	2×10^{-4}
3	7×10^{-5}	9×10^{-5}
4	8×10^{-5}	7×10^{-5}
5	2×10^{-5}	2×10^{-5}

Table 1(f)

a = 0.1; Non-uniform interval distribution

n	Global	Spline
	ε_{mod}	ε_{arg}
0	2×10^{-4}	2×10^{-3}
1	1×10^{-4}	5×10^{-5}
2	2×10^{-5}	3×10^{-6}
3	8×10^{-7}	5×10^{-7}
4	6×10^{-8}	2×10^{-7}
5	2×10^{-8}	8×10^{-8}

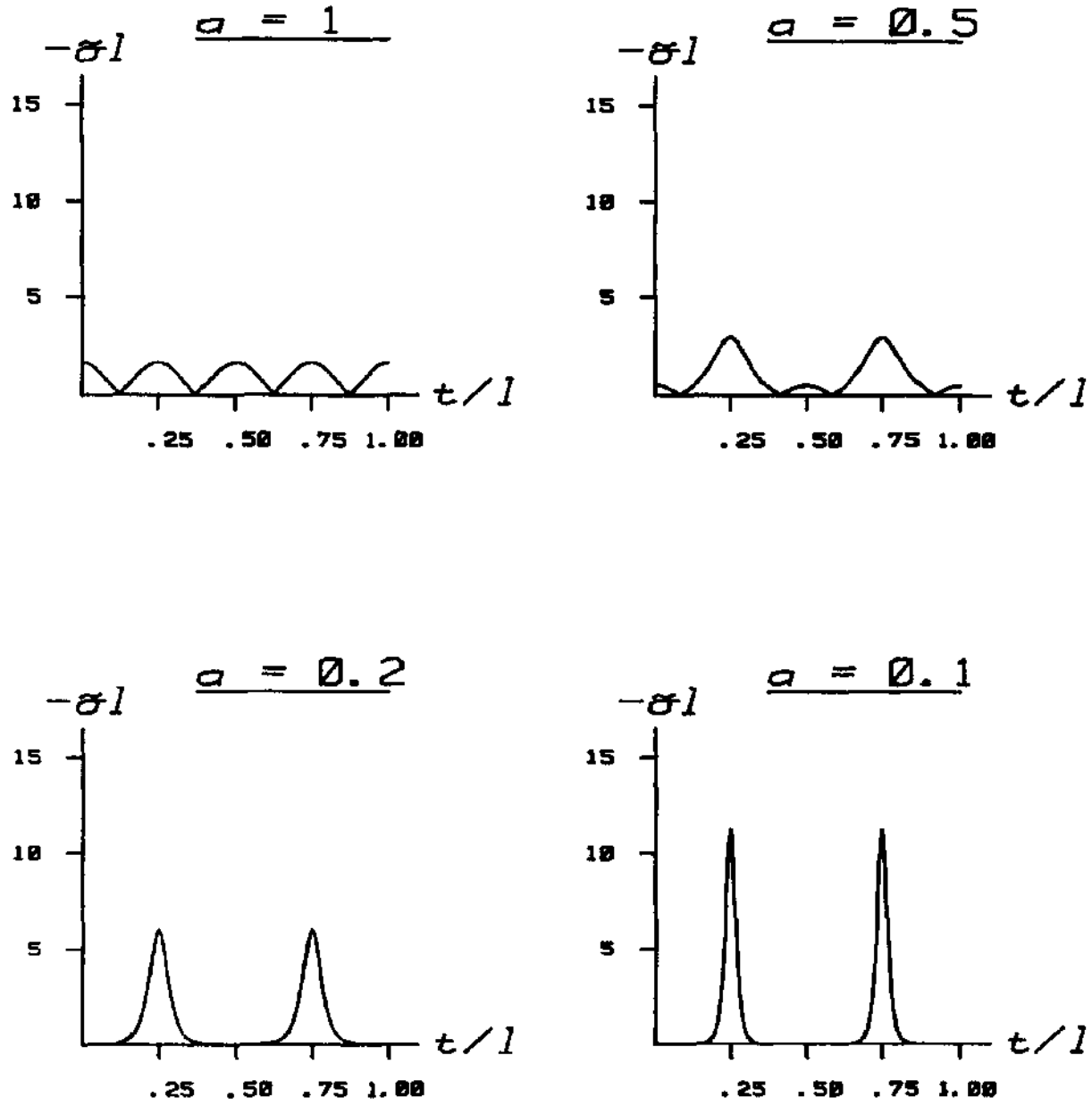

FIG. 1

$$\left\{\begin{array}{l} t/1 = 0,\ 0.5 \text{ correspond to the midpoints } z = \pm 1 \\ t/1 = 0.25,\ 0.75 \text{ correspond to the midpoints } z = \pm i\,a \end{array}\right\}$$

Example 2 L-Shape Region ; Figure 2.

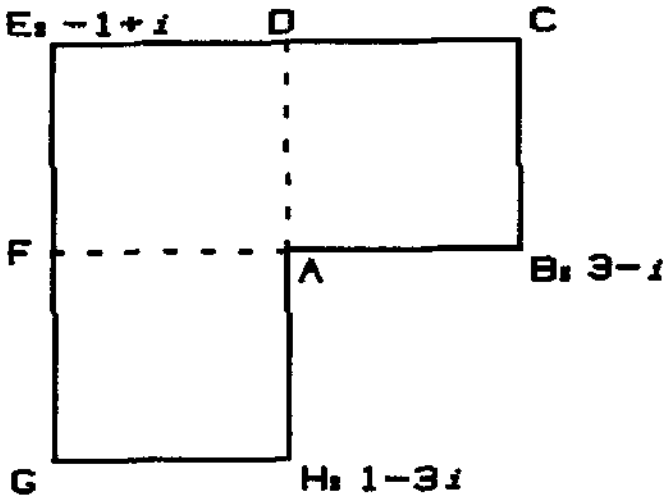

FIG. 2

In the numerical method we take

$$m_B = m_C = m_E = m_G = m_H = m \quad ,$$

and use 128 intervals of uniform length over the whole boundary. Because of the symmetry of the region about the line AE, the number of collocation equations and the total number of equations can be reduced respectively to M_1^* , M_0^* where

$$M_1^* = \begin{cases} 65 , & n \text{ odd} \quad , \\ 64 , & n \text{ even} \quad , \end{cases}$$

$$M_0^* = \begin{cases} M_1^* + [m_A/2] + [m/2] + 3n + (m_A + 5m)/2 - 6 , & m_A \neq 0 \text{ and } m \neq 0 \\ M_1^* + + 2[n/2] & , m_A = m = 0 \ . \end{cases}$$

Numerical results are presented in Tables 2(a), 2(b). In Table 2(a) we give the computed values of ε_{mod} and in Table 2(b) we give the errors in the computed values of the three cross-ratios corresponding respectively

to the "quadrilaterals" BCEG, ABDH and BEGH; see Gaier [4]. The exact mapping function is not known in this case. However, the exact values of the cross-ratios are derived in Gaier [3]. Also, in [4] the values computed by the method of Hayes et al [5] are presented.

For all the augmented spline results we fix m at either 2 or 3, depending on whether n is even or odd, and then consider all possible values for m . The results presented in Tables 2(a), 2(b) correspond to those values of m_A. which give the smallest values of ε_{mod} . In all cases the maximum error ε_{mod} , occurs in the neighbourhood of the re-entrant corner. We note that this example is also considered in Levin et al [103, who use a numerical method based on the Bergman kernel function of the domain . Their estimate for the maximum error in modulus is 2×10^{-5}

Table 2(a)

Values of $\varepsilon_{mod.}$

n	Global Spline	Augmented Spline	m_A
0	3×10^{-2}	9×10^{-4}	2
1	1×10^{-2}	3×10^{-4}	3
2	3×10^{-2}	3×10^{-4}	4
3	2×10^{-2}	4×10^{-5}	3
4	3×10^{-2}	3×10^{-5}	4
5	2×10^{-2}	2×10^{-5}	3

Table 2(b)

Errors in Cross—Ratios .

Degree of Augmented Spline	Quadrilateral		
	BCEG	ABDH	BEGH
0	5×10^{-6}	2×10^{-3}	6×10^{-6}
1	1×10^{-5}	9×10^{-5}	1×10^{-5}
2	2×10^{-6}	6×10^{-5}	3×10^{-6}
3	4×10^{-9}	7×10^{-7}	5×10^{-9}
4	3×10^{-7}	7×10^{-6}	3×10^{-7}
5	2×10^{-7}	4×10^{-6}	2×10^{-7}
Symm*	3×10^{-4}	8×10^{-3}	3×10^{-4}
Hayes et al **	3×10^{-4}	7×10^{-3}	3×10^{-4}

* i.e., the global spline n=0.

** These results are given in Gaier [4, p. 128] and are obtained by using 128 collocation points.

Example 3 The region shown in Figure 3.

In the numerical method we take

$$m_A = m_D = m_F = m_1, \qquad m_B = m_C = m_G = m_H = m_2,$$

and use 128 intervals over the whole boundary, with 32 intervals on DF and 16 intervals on all the other sides. On each side the intervals are of equal length. Because of the symmetry of the region about the line AE the number of collocation equations and the total number of equations

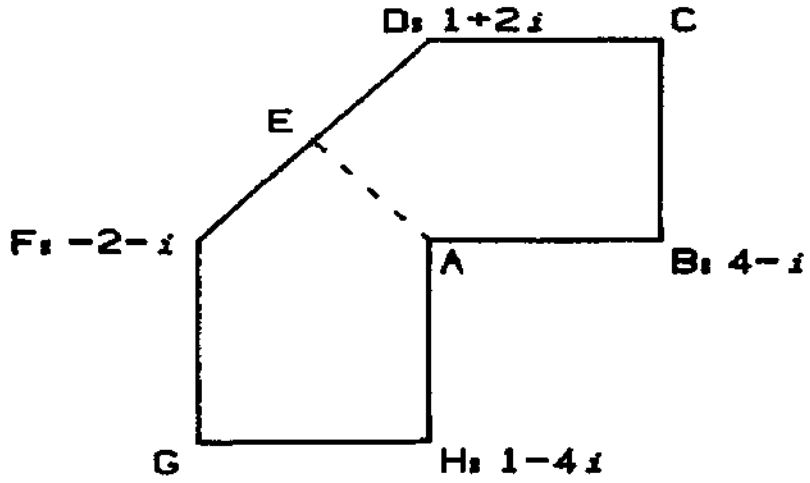

FIG. 3

can be reduced respectively to M_1^* , M_0^* where

$$M_1^* = \begin{cases} 65, & n \text{ odd}, \\ 64, & n \text{ even}, \end{cases}$$

$$M_0^* = \begin{cases} M_1^* + [m_1/2] + [n/2] + 7n/2 + 3m_1/2 + 2m_2 - 7, & m_1 \neq 0 \text{and} m_2 \neq 0 , \\ M_1^* + [m_1/2] + [n/2] + 3n/2 + 3m_1/2 - 3 , & m_1 \neq 0 \text{and} m_2 = 0 , \\ M_1^* + 2[n/2] , & m_1 = m_2 = 0 . \end{cases}$$

Numerical results are presented in Table 3 where we give the computed value of ε_{mod} . For the augmented splines these results are obtained using the following values ,

$$m_1 = \begin{cases} 2, & n = 0 \\ 3, & n = 1,3,5 \\ 4, & n = 2,4 , \end{cases}$$

$$m_2 = \begin{cases} 0, & n = 0,1 \\ 2, & n = 2,4 \\ 3, & n = 3,5 \end{cases} .$$

In all cases the maximum error ε_{mod} . occurs in the neighbourhood of the re-entrant corner. By comparison, the Bergman kernel method of [10] gives 3x10 as an estimate for the maximum error in modulus; see Papamichael and Sideridis [12, Ex.2.5] .

Table 3

Values of ε_{mod}

n	Global Spline	Augmented Spline
0	4×10^{-2}	2×10^{-3}
1	2×10^{-2}	4×10^{-4}
2	4×10^{-2}	5×10^{-4}
3	2×10^{-2}	8×10^{-5}
4	4×10^{-2}	2×10^{-4}
5	2×10^{-2}	6×10^{-5}

Example 4 The region shown in Figure 4.

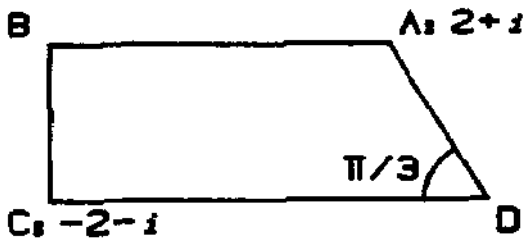

FIG. 4

In this case an explicit formula approximating the mapping function is obtained in [12, Ex. 2.1] . In the numerical method we take

$$m_B = m_C = m$$

and, since σ has no singularities at a $\pi/3$ corner, we set

$$m_D = 0$$

For the boundary discretization we use 128 intervals over the whole boundary taking 24, 40, 16 and 48 intervals respectively on DA, AB, BC and CD. On each side the intervals are of equal length.

Numerical results are presented in Tables 4(a) and 4(b). In Table 4(a) we give the computed values of ε_{mod} for augmented splines using the values

$$m_3 = \begin{cases} 0, & n = 1 \\ 2, & n = 0,2 \\ 3, & n = 3,5 \\ 4, & n = 4 \end{cases},$$

$$m_3 = \begin{cases} 0, & n = 0,1 \\ 2, & n = 2,4 \\ 3, & n = 3,5 \end{cases}.$$

The maximum error in modulus ε_{mod} occurs at C for $n = 0$, at the test point nearest $z = -i$ for $n = 1$, and in the neighbourhood of A for $n \geq 2$. By comparison the method of Levin et al [10] gives 5×10^{-7} as an estimate for the maximum error in modulus.

In Table 4(b) we give the real and imaginary parts of the approximation $\tilde{f}$ corresponding to

$$n = 3 , \quad m_A = m = 3 .$$

We compare these results with their counterparts computed from the approximate mapping function $\hat{f}$ given in [12].

Table 4(a)

Values of ε_{mod}

n	Augmented Spline
0	3×10^{-4}
1	4×10^{-5}
2	1×10^{-6}
3	8×10^{-7}
4	4×10^{-7}
5	1×10^{-7}

Table 4(b) *

z	Re($\tilde{f}$)	Im($\tilde{f}$)	Re($\hat{f}$)	Im($\hat{f}$)
-2 + i	-C.9856084	0.1690445	-0.9856086	0.1690442
i	0.0000000	1.0000000	0.0000000	1.0000002
2 + i	0.9923969	0.1230790	0.9923964	0.1230788
-1 + i/2	-0.7225487	0.2297512	-0.7225487	0.2297513
1 + i/2	0.7171559	0.2245559	0.7171559	0.2245559
-2	-0.9999961	-0.0028092	-0.9999959	-0.0028090
2+ 1/√3	0.9998057	-0.0197103	0.9998059	-0.0197106
-1 – i /2	-0.7212457	-0.2338070	-0.7212457	-0.2338069
1 - i / 2	0.7179986	-0.2204017	0.7179986	-0.2204018
-2 - i	-0.9846431	-0.1745795	-0.9846435	-0.1745796
- i	0.0056429	-0.9999839	0.0056431	-0.9999843
2 - i	0.9950346	-0.0995298	0.9950342	-0.0995302
2+2/√3-i	0.9983463	-0.0574871	0.9983468	-0.0574865

*

The unit circle in the w-plane is oriented such that $\arg(\tilde{f}(i)) = \arg(\hat{f}(i)) = \pi/2$.

5. Discussion

We make the following general comments regarding the implementation and applicability of the method.

As is well known, the truncated power function representation (3.5) can lead to ill-conditioned linear systems. For splines and augmented splines of degree $n < 3$ there appear to be no ill-conditioning problems in solving the linear system for the parameters of our approximation. However, in almost all examples, the subroutine for the solution of the linear system returns a warning message indicating possible loss of significance for $n > 4$. This suggests that for high degree splines, especially if the knot spacing is non-uniform, the use of the B-spline representation instead of (3.5) might be necessary.

On the basis of our numerical results it would be difficult to fully justify a general recommendation regarding the choice of the approximating function $\tilde{\sigma}$. However, our experiments suggest that a reasonable strategy is to use augmented cubic splines with 3 singular terms for each singular corner. This leads to C^1 continuity at the transition points. Furthermore, for ease of application, it might be preferrable to treat every corner of a polygon as a "singular corner"; i.e. at every corner introduce appropriate terms from the series (3.4).

Clearly the method of this paper can be generalized to regions with curved boundaries. The main difficulty for this concerns the accurate evaluation of the integrals corresponding to (3.21). In the case of curved boundaries, such integrals must be evaluated by numerical quadrature. Although Gaussian formulae provide good approximations to the non-singular integrals, special treatment is necessary for any logarithmic and fractional power singularities.

Corner singularities are not the only source for inaccuracies in the numerical method. As the mapping of the thin rectangle considered in Example 1 shows, if the mapping function has a pole which lies near the boundary $\partial\Omega$ then, in the neighbourhood of this singularity, it may be difficult to approximate σ accurately be means of spline functions with equally spaced knots. In the case of the thin rectangle the difficulties associated with the poles of f(z) were largely overcome by a suitable choice of knot spacing. This procedure can clearly be used in other cases. Alternatively, we believe that the possibility of introducing appropriate functions which reflect the "singular" behavious of σ near a pole is a problem that deserves serious consideration .

REFERENCES

[1] Copson, E.T.: Partial Differential Equations, London: Cambridge University Press 1975.

[2] Gaier, D. : Konstruktive Methoden der konformen Abbildung. Berlin-Gottingen-Heidelberg: Springer 1964 .

[3] Gaier, D.: Ermittlung des konformen Moduls von Vierecken mit Differenzenmethoden. Numer. Math. 19, 179-194 (1972).

[4] Gaier, D.: Integralgleichungen erster Art und konforme Abbildung. Math. Z. 147, 113-129 (1976).

[5] Hayes, J.K., Kahaner, D.K., and Kellner, R.G.: An improved method for numerical conformal mapping. Math. Comp. 26, 327-334 (1972).

[6] Hayes, J.K., Kahaner, D.K., and Kellner, R.G.: A comparison of integral equations of the first and second kind for conformal mapping. Math. Comp. 29 , 512-521 (1975).

[7] Henrici, P,: Fast Fourier methods in computational complex analysis. SIAM Review, 21 481-527 (1979).

[8] Hough, D.M.: Exact formulae for certain integrals arising in potential theory. Technical Report TR/98, Dept. of Maths, Brunei University, 1980.

[9] Jaswon, M.A, and Symm, G.T.: Integral equation methods in potential theory and elastostatics. London: Academic Press 1977.

[10] Levin, D., Papamichael, N. and Sideridis, A.: The Bergman kernel method for the numerical conformal mapping of simply connected domains. J. Inst. Maths Applies, 22, 171-187 (1978).

[11] Milne-Thomson, L.M.: Jacobian elliptic function tables. New York: Dover Publications 1950.

[12] Papamichael, N. and Sideridis, A.; Formulae for the approximate conformal mapping of some simply connected domains. Technical Report TR/72, Dept of Maths, Brunei University 1977.

[13] Symm, G.T.: An integral equation method in conformal mapping. Numer. Math. 9, 250-258 (1966).

[l4] Symm, G.T. a Problems in two-dimensional potential theory. Numerical Solution of integral equations. (Ed. L.M. Delves and J. Walsh). Oxford: Clarendon Press 1974.

[15] Symm, G.T.: The Robin problem for Laplace's equation. New developments in boundary element methods (Ed. C.A. Brebbia) CML Publications 1980.

[16] Wendland, W.L.: On Galerkin collocation methods for integral equations of elliptic boundary value problems. To appear.